

Lev Truskinovsky · Anna Vainchtein

Quasicontinuum models of dynamic phase transitions

Received: 15 July 2005 / Accepted: 10 March 2006 / Published online: 5 May 2006
© Springer-Verlag 2006

Abstract We propose a series of quasicontinuum approximations for the simplest lattice model of a fully dynamic martensitic phase transition in one dimension. The approximations are dispersive and include various non-classical corrections to both kinetic and potential energies. We show that the well-posed quasicontinuum theory can be constructed in such a way that the associated closed-form kinetic relation is in an excellent agreement with the predictions of the discrete theory.

Keywords Quasicontinuum approximations · Martensitic phase transitions · Kinetic relations · Lattice models · Nonlocal interactions · Gradient models · Microkinetics · Configurational forces

PACS 64.70.Kb, 61.72.Bb, 63.90.+ t

1 Introduction

A recent trend in replacing continuum mechanical phenomenology with microscopic simulations raised an interest in developing lattice models for propagating defects (e.g. [2, 12, 16, 24, 33] and the literature cited therein). The large nonlinear systems of ordinary differential equations used in such studies are rather complex and are typically not amenable to a detailed parametric analysis. Continuum theories, which assume that the lattice parameter is equal to zero, are much more transparent than their discrete prototypes. However, in order to handle defects they still require external phenomenological closing relations governing the dynamics of the associated singularities.

Since away from the singularities (defects) conventional continuum theories deliver reasonably accurate reproduction of the behavior of the underlying discrete models, efforts have been made to augment the classical description in the core region of the defects by bringing into continuum models terms that describe behavior at short wave lengths. The resulting models can be called quasicontinuum since unlike the truly continuum theories they explicitly account for the cutoff distance. Among the most well known examples of the quasicontinuum models are strain-gradient elasticity, incorporating into the energy function higher derivatives of

Communicated by A. DeSimone

L. Truskinovsky
Laboratoire de Mécanique des Solides, CNRS-UMR 7649,
Ecole Polytechnique, 91128, Palaiseau, France
E-mail: trusk@lms.polytechnique.fr

A. Vainchtein (✉)
Department of Mathematics, University of Pittsburgh,
Pittsburgh, PA 15260, USA
E-mail: aav4@pitt.edu

displacements (e.g. [17,27]), and fully nonlocal theory of elasticity leading to a formulation in terms of integral equations (e.g. [14,19]). While in linear regime the relation between the corresponding discrete, continuum and quasicontinuum theories can be considered rather well understood (e.g. [7]), the situation with nonlinear regimes is far from being clear, as indicated, for instance, by the status of the discrete approximations in the general theory of hyperbolic equations (e.g. [15]). The problem is even more difficult when the essential nonlinearity manifests itself through the loss of convexity of the energy. This is exactly what happens in the situations involving formation and propagation of defects in solids.

More specifically, in the discrete problems with nonconvex energy the long-wave continuum approximations develop singularities whose dynamics remains largely arbitrary. This leads to nonuniqueness and requires an additional input from the discrete theory. To overcome this problem, one can focus on a quasicontinuum, rather than continuum, approximation which combines the advantages of a homogenized description with an ability to capture the important physics at small scales. To test the effectiveness of such quasicontinuum theories it is natural to begin by studying the motion of an isolated defect, which may be a dislocation, a crack tip or a phase boundary.

Given that the dynamics of all these defects exhibit considerable similarities (e.g. [13]) we focus in this paper on a martensitic phase boundary as the simplest example of a singularity that can be adequately described already in one dimension. Similar to shocks, martensitic phase boundaries are modeled at the continuum level as propagating strain discontinuities. However, unlike shocks, they require for their unique determination an explicit specification of the rate of dissipation. This is usually accomplished by complementing the system of Rankine-Hugoniot jump conditions by a *kinetic relation* which links the driving force acting on a phase boundary with its velocity [1,29]. Lattice models generate such relations automatically due to the phenomenon of radiative damping (e.g. [10]).

In the present paper we illustrate the above point in the framework of a prototypical lattice model amenable to a fully analytical treatment. This model has been originally introduced in [32,33] as a natural development of the earlier models (e.g. [25]) which have shown some undesirable degeneracy. The main goal of this paper is to reproduce the exact discrete kinetic relation generated by the lattice model (see [32,33]) by employing various quasicontinuum approximations. Our main result is a series of simple and explicit functions approximating exact kinetic relations that can be effectively used as admissibility conditions for the long-wave continuum models.

In more detail, we develop a set of improving quasicontinuum approximations for a one-dimensional fully inertial lattice with bi-stability and long-range interactions. An important feature of our quasicontinuum models is that the associated energy functionals contain higher-order spatial derivatives of both strain and velocity fields, introducing dispersive corrections to both kinetic and potential energies. In the general context of lattice theories, the approximations of this type have been originally proposed by Rosenau [20–22] who followed some important earlier insights presented in [3,5]. A more recent development of these ideas in the context of solitary waves in lattices can be found in [8,9,35–37]. In the phenomenological continuum theories velocity gradients have been previously incorporated into kinetic energy in the theory of rods [18], models of bubbly fluids [4,6] and in the description of solids with “microkinetic” energy [26]. We follow this tradition and conclude that the quasicontinuum approximations accounting for both strain and velocity gradients are remarkably successful in generating closed-form kinetic relations in full agreement with the predictions of the discrete theory. We also show how such approximations can be constructed without sacrificing the well-posedness of an initial value problem, which has always been an unpleasant signature of the straightforward quasicontinuum theories based on higher strain gradients only.

The structure of the paper is as follows. In Sect. 2 we briefly review the phenomenological origin of kinetic relations in the continuum theory of dynamic phase transitions. We then introduce in Sect. 3 a prototypical discrete model which leads to a canonical advance-delay differential equation governing the dynamics of an isolated phase boundary. In Sect. 4 we present a nonstandard reformulation of the discrete problem as a continuum problem with a strong spatial nonlocality of both kinetic and potential energies. Various quasicontinuum approximations based on either Taylor or Padé approximations of the corresponding kernels are presented in Sect. 5. In Sect. 6 we use Fourier transform to obtain a series of analytical solutions for the traveling waves in the discrete and quasicontinuum problems. In Sect. 7 we show how to extract from a fully conservative solution of the discrete/quasicontinuum problem a kinetic relation governing the rate of dissipation at the continuum scale. Examples of quasicontinuum approximations generating explicit kinetic relations are discussed in Sect. 8, where we also provide a detailed comparison of the resulting kinetics with the exact solution for the discrete theory. Finally, in Sect. 9 we discuss the issue of well-posedness of the truncated quasicontinuum

approximations and offer a rather universal way of dealing with unboundedness of the approximate operators at short wave lengths. Our conclusions are presented in Sect. 10.

2 Continuum model

To present our ideas in the simplest setting, consider longitudinal motions of a homogeneous elastic bar with the total energy

$$\mathcal{E} = \int \left[\frac{\rho \dot{u}^2}{2} + \phi(u_x) \right] dx, \quad (1)$$

where $u(x, t)$ is the displacement field, $\dot{u} \equiv \partial u / \partial t$ is the velocity, $u_x \equiv \partial u / \partial x$ is the strain, ρ is the constant mass density, and $\phi(u_x)$ is the elastic energy density. When the motion is smooth, the function $u(x, t)$ satisfies the nonlinear wave equation

$$\rho \ddot{u} = (\sigma(u_x))_x, \quad (2)$$

where $\sigma(u_x) = \phi'(u_x)$ is the stress-strain relation. The parameters on a discontinuity moving with velocity V must satisfy both the classical Rankine-Hugoniot jump conditions

$$[[\dot{u}]] + V[[u_x]] = 0, \quad \rho V[[\dot{u}]] + [[\sigma(u_x)]] = 0,$$

and the entropy inequality $\mathcal{R} = GV \geq 0$, where \mathcal{R} is the rate of dissipation and

$$G = [[\phi]] - \{\sigma\}[[u_x]] \quad (3)$$

is the configurational (driving) force. Here $[[f]] \equiv f_+ - f_-$ denotes the jump and $\{f\} \equiv (f_+ + f_-)/2$ - the average of f across the discontinuity.

Unlike conventional shocks, subsonic discontinuities violate the Lax condition. The resulting nonuniqueness can be remedied by supplementing the above jump conditions by a kinetic relation specifying the dependence of the configurational force on the velocity of the phase boundary $G = G(V)$ [1,29]. Note that the continuum model provides no information about this function. One way to recover the kinetic relation is to consider a lattice model representing physically justified ‘‘dehomogenization’’ of the continuum model (2).

3 Discrete model

As a micro-model for a bar undergoing phase transition, consider an infinite chain of particles, each interacting with q nearest neighbors on both sides. The total energy of the system may be written as

$$\mathcal{E} = \varepsilon \sum_{n=-\infty}^{\infty} \left[\frac{\rho \dot{u}_n^2}{2} + \sum_{p=1}^q p \phi_p \left(\frac{u_{n+p} - u_n}{p\varepsilon} \right) \right], \quad (4)$$

Here $u_n(t)$ is the displacement of the n th particle, \dot{u}_n is the particle velocity, ε is the reference interparticle distance, ρ is the mass density and $\phi_p(w)$ is the energy density of the interaction between p th nearest neighbors (meaning that the energy is normalized by the reference length of the corresponding bond).

To represent martensitic phase transitions in the simplest way we may assume that the nearest-neighbor (NN) interactions are governed by a bi-parabolic potential representing an example of the simplest essential nonlinearity:

$$\phi_1(w) = \begin{cases} \frac{1}{2}\Psi(1)w^2, & w \leq w_c, \\ \frac{1}{2}\Psi(1)(w - a)^2 + a\Psi(1)\left(w_c - \frac{a}{2}\right), & w \geq w_c, \end{cases} \quad (5)$$

Here $\Psi(1)$ is the short range elastic modulus which is assumed to be the same in both phases. One can see that the nonlinear springs representing NN interactions can be found in two different states depending on whether the strain w is below (phase I) or above (phase II) the critical strain $w_c > 0$; the constant term in (5) ensures

the continuity of the energy at $w = w_c$. Parameter $a > 0$ is the microscopic transformation strain which is independent of w_c . The potentials governing long-range interactions are assumed to be quadratic:

$$\phi_p(w) = \frac{1}{2} p \Psi(p) w^2, \quad p = 2, \dots, q, \quad (6)$$

where $\Psi(p)$ is the elastic modulus of p th interaction.

Next we introduce the dimensionless variables

$$\begin{aligned} \bar{t} &= \frac{t}{\varepsilon} \left(\frac{\Psi(1)}{\rho} \right)^{1/2} & \bar{u}_n &= \frac{u_n}{a\varepsilon} & \bar{w}_c &= \frac{w_c}{a}, \\ \bar{\Psi}(p) &= \frac{\Psi(p)}{\Psi(1)} & \bar{\mathcal{E}} &= \frac{\mathcal{E}}{\varepsilon \Psi(1) a^2}. \end{aligned}$$

We then drop the bars and rewrite in the new variables the total energy of the chain

$$\mathcal{E} = \sum_{n=-\infty}^{\infty} \left[\frac{\dot{u}_n^2}{2} - \frac{1}{2} \sum_{|k-n| \leq q} u_n \Psi(k-n) u_k - (w_n - w_c) \theta(w_n - w_c) \right]. \quad (7)$$

Here $w_n = u_n - u_{n-1}$ is the strain in NN springs, and $\theta(w)$ is a unit step function ($\theta(w) = 1$ if $w \geq 0$ and zero otherwise). In (7) we have defined

$$\Psi(0) = -2 \sum_{p=1}^q \Psi(p), \quad \Psi(-p) = \Psi(p) \quad (8)$$

The dynamic equations can now be formulated for the strain variables w_n :

$$\ddot{w}_n - \sum_{|k-n| \leq q} \Psi(k-n) w_k = 2\theta(w_n - w_c) - \theta(w_{n+1} - w_c) - \theta(w_{n-1} - w_c). \quad (9)$$

Note that in the classical continuum limit the discrete model converges to the rescaled equations (1), (2) with $\rho = 1$ and the bilinear macroscopic stress given by

$$\sigma(w) = c^2 w - \theta(w - w_c), \quad (10)$$

where

$$c^2 = \sum_{p=1}^q p^2 \Psi(p) \quad (11)$$

is the dimensionless macroscopic sound speed; see Fig. 1.

To model the motion of an isolated phase boundary, we now consider solutions of (9) in the form of the traveling waves $w_n(t) = w(\xi)$, $\xi = n - Vt$, with all springs are in phase I ($w < w_c$) for $\xi > 0$ and in phase II ($w \geq w_c$) otherwise. For these solutions the system of Eq. (9) reduces to a single advance-delay differential equation for $w(x)$:

$$V^2 w'' - \sum_{|p| \leq q} \Psi(p) w(\xi + p) = 2\theta(-\xi) - \theta(-\xi - 1) - \theta(1 - \xi). \quad (12)$$

We observe that for the class of solutions under consideration the the original nonlinear equation has been replaced by a linear equation with a given right hand side. This simplification is the main reason one can obtain an explicit solution for the piecewise linear model.

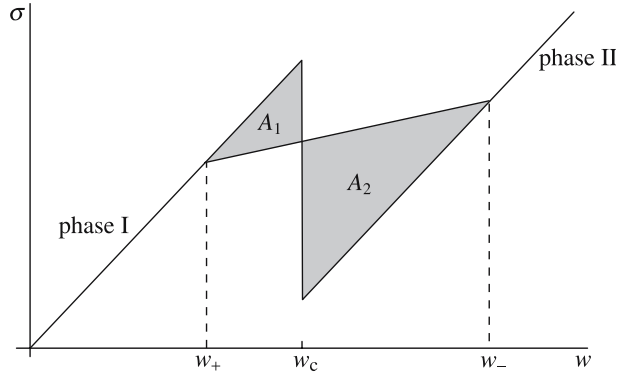


Fig. 1 The bilinear macroscopic stress-strain law and the Rayleigh line connecting the states at infinity for a traveling wave solution describing an isolated phase boundary. The difference between the shaded areas $A_2 - A_1$ represents the configurational force G

4 Reformulation of the problem

Observe that Eq. (12) may be written in the form

$$\Lambda^D(w - w_+) = \theta(-\xi), \quad (13)$$

where w_+ is a constant that will be later identified with the constant strain at plus infinity, and the operator Λ^D is defined by

$$\Lambda^D \equiv -\Delta_d^{-1} \left(V^2 \Delta_c - \sum_{|p| \leq q} \Psi(p) \exp(pD) \right). \quad (14)$$

Here D is the operator of differentiation, $Dw = w_\xi$. We further defined the continuum Laplacian operator $\Delta_c = D^2$ and the shift operator $\exp(pD)$ acting according to $\exp(pD)w = w(\xi + p)$. Finally, $\Delta_d = \exp(D) - 2I + \exp(-D)$ is the discrete Laplacian, defined by its action on w as

$$\Delta_d w = w(\xi + 1) - 2w(\xi) + w(\xi - 1).$$

The Fourier image of (14) is given by

$$\Lambda^D(k, V) = \frac{\omega^2(k) - V^2 k^2}{4 \sin^2(k/2)}, \quad (15)$$

where

$$\omega^2(k) = 4 \sum_{p=1}^q \Psi(p) \sin^2 \frac{pk}{2}. \quad (16)$$

is the dispersion relation of the discrete model.

Following [22], we introduce a sufficiently smooth continuum displacement field $u(x, t)$ such that

$$\frac{\partial u}{\partial x}(n, t) \equiv u_n - u_{n-1}. \quad (17)$$

Notice that contrary to some common practices we approximate here the discrete strain field rather than the discrete displacement field. One can see that this assumption is equivalent to piecewise linear rather than piecewise constant approximation of the displacement field, which is crucial for the success of the ensuing quasicontinuum theory.

Using the standard notation for a shift operator $u_{n+1} = \exp(D)u_n$, this definition can be rewritten as

$$u_n(t) = \mathcal{M}u(n, t) \equiv (I - \exp(-D))^{-1} Du(n, t). \quad (18)$$

In most derivations of quasicontinuum approximations it is assumed that $\mathcal{M} = I$. To see the effect of this alternative definition of the continuum variable it is instructive to compute the kinetic energy. Let the operator \mathcal{K} be the continuum analog of the operator $\Delta_d^{-1} \Delta_c$, in the sense that their Fourier images coincide:

$$\mathcal{K}(k) = \mathcal{F}[\Delta_d^{-1} \Delta_c] = \frac{k^2}{4 \sin^2(k/2)}. \quad (19)$$

We can now use (17), (18), (19) and formally replace the sum in the expression for the kinetic energy

$$\frac{1}{2} \sum_{n=-\infty}^{\infty} \dot{u}_n(t) \cdot \dot{u}_n(t)$$

by the integral

$$\frac{1}{2} \int_{-\infty}^{\infty} \mathcal{M}u_t(x, t) \cdot \mathcal{M}u_t(x, t) dx = \frac{1}{2} \int_{-\infty}^{\infty} u_t(x, t) \mathcal{K}u_t(x, t) dx. \quad (20)$$

Observe that contrary to the more traditional approach (e.g. [14]), in our continuum variables the kinetic energy is nonlocal. By rewriting in the new variables the whole discrete energy (7) we obtain

$$\mathcal{E}_{QC} = \int_{-\infty}^{\infty} \left[\frac{1}{2} u_t \mathcal{K}u_t + \frac{1}{2} u_x \mathcal{L}u_x - (u_x - w_c) \theta(u_x - w_c) \right] dx, \quad (21)$$

where the operator \mathcal{L} is the continuum analog of $\Delta_d^{-1} \sum_{|p| \leq q} \Psi(p) \exp(pD)$, in the sense that

$$\mathcal{L}(k) = \mathcal{F} \left[\Delta_d^{-1} \sum_{|p| \leq q} \Psi(p) \exp(pD) \right] = \frac{\sum_{p=1}^q \Psi(p) \sin^2(pk/2)}{\sin^2(k/2)}. \quad (22)$$

The equation of motion generated by (21) is

$$\frac{\partial}{\partial t} [\mathcal{K}u_t] = \frac{\partial}{\partial x} [\mathcal{L}u_x - \theta(u_x - w_c)].$$

Applying the traveling wave ansatz $u(x, t) = \tilde{u}(\xi)$, $\xi = x - Vt$ and integrating the resulting equation, we obtain

$$(\mathcal{L} - V^2 \mathcal{K})w - \theta(w - w_c) = \text{const},$$

where $w(\xi) = \tilde{u}'(\xi)$ is the strain. Now, assuming as in (12) that $\theta(w - w_c) = \theta(-\xi)$ and applying the boundary condition $w \rightarrow w_+$ as $\xi \rightarrow \infty$, we arrive at

$$(\mathcal{L} - V^2 \mathcal{K})(w - w_+) = \theta(-\xi), \quad (23)$$

Note that (23) is the exact analog of (13) due to the identity

$$\Lambda^D(k, V) = \mathcal{L}(k) - V^2 \mathcal{K}(k). \quad (24)$$

The continuum model with the energy (21) is equivalent to the discrete model with the energy (7). Notice that in contrast to the quasicontinuum models proposed in [14], which preserve the structure of the kinetic energy while modifying only the elastic energy, we propose to modify expressions for both kinetic and elastic energies. This reflects the physical understanding that the microscopic lattice-scale vibrations cannot be treated at the mesoscale exclusively as thermodynamic free energy. Here we follow a tradition which dates back to Rayleigh who in his studies of vibrating beams understood the necessity of incorporating the concept of transversal inertia [18]. Similar ideas appeared in many areas, for instance in the homogenized theory of bubbly fluids where the extra terms in the kinetic energy describe inertia of individual bubbles [4,6].

5 Quasicontinuum approximations

The quadratic part of the nonlocal functional (21) can be approximated by local functionals in several ways. This gives rise to significantly different quasicontinuum theories.

5.1 Strain-gradient approximation

The most common way of approximating discrete energy functional is based on retention of only the non-dispersive continuum expression for the kinetic energy. This means that the operator $\mathcal{K} = \Delta_d^{-1} \Delta_c$ (see (19)) is replaced by I , which is equivalent to replacing the discrete Laplacian Δ_d by Δ_c . For consistency the operator \mathcal{L} should then be replaced by $\Delta_c^{-1} \sum_{|p| \leq q} \Psi(p) \exp(pD)$. Expanding the Fourier image of the resulting approximate operator in Taylor series around $k = 0$ and retaining the first few terms, we obtain

$$\mathcal{K}(k) \approx 1, \quad \mathcal{L}(k) \approx c^2 + \alpha_1 k^2 + \alpha_2 k^4, \quad (25)$$

where

$$\alpha_1 = -\frac{1}{12} \sum_{p=1}^q p^4 \Psi(p), \quad \alpha_2 = \frac{1}{360} \sum_{p=1}^q p^6 \Psi(p). \quad (26)$$

Observe that in the physical space the associated quadratic part of potential energy reduces to

$$\frac{1}{2} \int_{-\infty}^{\infty} u_x \mathcal{L} u_x dx \approx \frac{1}{2} \int_{-\infty}^{\infty} [c^2 u_x^2 + \alpha_1 u_{xx}^2 + \alpha_2 u_{xxx}^2] dx.$$

This approximation is often referred to as the strain-gradient (SG) model (e.g. [17,28]). Its advantage is relative simplicity. However, the Fourier image of the approximate operator agrees with $\Lambda^D(k, V)$ only up to $O(k^2)$. This order of approximation is shared even by strongly nonlocal quasicontinuum models that are focused exclusively on the approximation of the elastic energy (e.g. [14,19]).

5.2 Mixed gradient approximation

To obtain a higher order of approximation one must include the dispersive corrections in both kinetic and elastic energies. For instance, by expanding the Fourier images (19), (22) of the two operators \mathcal{K} and \mathcal{L} to the same order in Taylor series we obtain

$$\mathcal{K}(k) \approx 1 + \frac{k^2}{12} + \frac{k^4}{240}, \quad \mathcal{L}(k) \approx c^2 + a_1 k^2 + a_2 k^4, \quad (27)$$

where

$$a_1 = \frac{1}{12} \sum_{p=2}^q (p^2 - p^4) \Psi(p), \quad a_2 = \frac{1}{720} \sum_{p=2}^q p^2 (3 - 5p^2 + 2p^4) \Psi(p). \quad (28)$$

In this approximation the kinetic energy and the quadratic part of the potential energy take the form

$$\begin{aligned} \frac{1}{2} \int_{-\infty}^{\infty} u_t \mathcal{K} u_t dx &\approx \frac{1}{2} \int_{-\infty}^{\infty} \left[u_t^2 + \frac{1}{12} u_{xt}^2 + \frac{1}{240} u_{xxt}^2 \right] dx, \\ \frac{1}{2} \int_{-\infty}^{\infty} u_x \mathcal{L} u_x dx &\approx \frac{1}{2} \int_{-\infty}^{\infty} \left[c^2 u_x^2 + a_1 u_{xx}^2 + a_2 u_{xxx}^2 \right] dx. \end{aligned} \quad (29)$$

We will refer to this class of models as mixed gradient (MG) models.

An approximation of this type with only quadratic term in k preserved in the kinetic energy and only zero-order term retained in the elastic energy have been proposed by Rosenau [20]. These ideas were further developed in [8,9,12,22,23,35–37], where various rational approximations of the discrete operator are considered.

The advantage of the Rosenau model is that it is uniformly well-posed in the sense that it avoids unphysical short-wave instabilities that are characteristic for generic truncated polynomial approximations. This issue will be addressed in more detail in Sect. 9, while here we simply mention that by well-posedness we mean the discrete analog of hyperbolicity of the linear operator of the model in the sense that $\omega^2(k) = k^2 \mathcal{L}(k)/\mathcal{K}(k)$ is positive for all nonzero k (see [11] for more detail).

To construct an improved Rosenau approximation with a higher resolution we assume that $\mathcal{L}(k)$ and $\mathcal{K}(k)$ are still approximated by polynomials. Then the MG model leads to a well-posed problem if (1) the approximation of $\mathcal{L}(k)$ has no real zeroes and (2) $k^2 \mathcal{L}(k)$ and $\mathcal{K}(k)$ are approximated by polynomials of the same order. This leads to the next simplest Rosenau-type well-posed model

$$\mathcal{K}(k) \approx 1 + \frac{k^2}{12} + \frac{k^4}{240}, \quad \mathcal{L}(k) \approx c^2 + a_1 k^2 \quad (30)$$

with a_1 as in (28). Both of the above requirements are satisfied provided that $a_1 > 0$, so that $c^2 + a_1 k^2 = 0$ has no real roots. Note that unlike the general MG model (27), where both kinetic and elastic operators are expanded up to $O(k^6)$, this model approximates the discrete operator only up to $O(k^4)$ because of lower order accuracy in approximating $\mathcal{L}(k)$. In what follows we refer to the model (30) as MG1/2 model because of its intermediate character.

5.3 Mixed gradient-Padé approximation

Another possibility to preserve the well-posedness of the linear problem is to approximate $\mathcal{L}(k)$ by a (2, 2) Padé (rational) approximation accurate up to $O(k^6)$, while keeping for $\mathcal{K}(k)$ a quadratic polynomial expansion:

$$\mathcal{K}(k) \approx 1 + \frac{k^2}{12}, \quad \mathcal{L}(k) \approx \frac{c^2 + b_1 k^2}{1 + b_2 k^2}, \quad (31)$$

with

$$b_1 = \frac{1}{12} \sum_{p=2}^q (p^2 - p^4) \Psi(p) - \frac{c^2 \sum_{p=2}^q p^2 (3 - 5p^2 + 2p^4) \Psi(p)}{60 \sum_{p=2}^q (p^2 - p^4) \Psi(p)}, \quad (32)$$

$$b_2 = - \frac{\sum_{p=2}^q p^2 (3 - 5p^2 + 2p^4) \Psi(p)}{60 \sum_{p=2}^q (p^2 - p^4) \Psi(p)}.$$

We will refer to this approximation as MGP model. In this case the dispersion relation (see (69)) remains to be the ratio of two polynomials of the same order, and if $b_1 > 0$, the MGP model leads to a well-posed problem. Note that like the well-posed version of the MG model (30), this approximation is accurate only up to $O(k^4)$. In this case it is due to the reduced accuracy in the expansion of $\mathcal{K}(k)$.

6 Traveling waves

The traveling wave equation for both discrete and quasicontinuum models can be written as

$$\Lambda(w - w_+) = \theta(-\xi), \quad (33)$$

where $\Lambda = \Lambda^D$ given in (14) for the discrete model,

$$\Lambda = (c^2 - V^2)I - \alpha_1 D^2 + \alpha_2 D^4 \quad (34)$$

for the SG model,

$$\Lambda = (c^2 - V^2)I - \left(a_1 - \frac{V^2}{12}\right)D^2 + \left(a_2 - \frac{V^2}{240}\right)D^4 \quad (35)$$

for the MG model and

$$\Lambda = (I - b_2 D^2)^{-1} (c^2 I - b_1 D^2) - V^2 \left(1 - \frac{1}{12} D^2 \right) \quad (36)$$

for the MGP model. For consistency with the assumptions that led to (33), we must also require that solution of equation (33) satisfies the following conditions:

$$w(0) = w_c, \quad (37)$$

ensuring the phase change at $\xi = 0$, and the constraints

$$w(\xi) < w_c \quad \text{for } \xi > 0, \quad w(\xi) \geq w_c \quad \text{for } \xi < 0, \quad (38)$$

which enforce the requirement that all springs are in phase II at $\xi < 0$ and phase I at $\xi > 0$. The average states at $\xi = \pm\infty$ must correspond to stable constant-strain equilibria

$$\langle w(\xi) \rangle \equiv \lim_{s \rightarrow \infty} \frac{1}{s} \int_{\xi}^{\xi+s} w(\zeta) d\zeta \rightarrow w_{\pm}, \quad \text{as } \xi \rightarrow \pm\infty. \quad (39)$$

We solve (33) by writing $w(\xi) = h(\xi) + w_+$ and applying the complex Fourier transform

$$\hat{h}(k) = \int_{-\infty}^{\infty} h(\xi) e^{i(k-i\alpha)\xi} d\xi, \quad h(\xi) = \frac{1}{2\pi} \int_{-\infty-i\alpha}^{\infty-i\alpha} \hat{h}(k) e^{-ik\xi} dk,$$

where $\alpha > 0$ is a small parameter which guarantees convergence of the integrals. After inverting the Fourier transform and letting $\alpha \rightarrow 0$, we obtain the integral representation

$$w(\xi) = w_+ - \frac{1}{2\pi i} \int_{\Gamma} \frac{e^{ik\xi}}{k\Lambda(k, V)} dk, \quad (40)$$

where the contour Γ coincides with the real axis everywhere except near the singular points. Specifically, it goes above $k = 0$ and, in order to satisfy the radiation condition, passes below the nonzero real roots of $\Lambda(k, V) = 0$ if the group velocity

$$V_g = \omega'(k) = V + \frac{k\Lambda_k(k, V)}{2V\mathcal{K}(k)} \quad (41)$$

exceeds V and above otherwise. In what follows, we will assume that $V > 0$ (the case $V < 0$ is treated similarly). Then the radiation condition reduces to requiring that the contour goes below a nonzero real root if $k\Lambda_k(k, V) > 0$ and above otherwise.

To compute the integral (40) explicitly, we use the residue method closing the contour in the upper half-plane when $\xi > 0$ and in the lower half-plane when $\xi < 0$. We obtain

$$w(\xi) = \begin{cases} w_- + \sum_{k \in M^-(V)} \frac{e^{ik\xi}}{k\Lambda_k(k, V)} & \text{for } \xi < 0 \\ w_+ - \sum_{k \in M^+(V)} \frac{e^{ik\xi}}{k\Lambda_k(k, V)} & \text{for } \xi > 0. \end{cases} \quad (42)$$

The average strains at $\pm\infty$ must satisfy a macroscopic Rankine-Hugoniot condition

$$w_+ = w_- - \frac{1}{c^2 - V^2}, \quad (43)$$

where we recall that c is the dimensionless macroscopic sound speed defined in (11). Note that since we assumed that $w_- < w_+$, the solutions are necessarily *subsonic* ($V < c$). The summations in (42) are over the sets of roots of $\Lambda(k, V) = 0$ defined as

$$M^\pm(V) = \{k : \Lambda(k, V) = 0, \operatorname{Im} k \gtrless 0\} \cup N^\pm(V),$$

where

$$N^\pm(V) = \{k : \Lambda(k, V) = 0, \operatorname{Im} k = 0, k\Lambda_k(k, V) \gtrless 0\}$$

are the sets of real roots responsible for radiative modes whose amplitude does not decrease at infinity. These waves are placed either behind or in front of the moving phase boundary according to the radiation condition. Observe that by construction all plane waves with real wave numbers k involved in the traveling wave solution (33) have real frequency $\omega(k) = Vk$, so they lie inside the region in Fourier space where the models are well-posed.

The smoothness of the obtained solution (42) at $\xi = 0$ depends on the asymptotic behavior of $\Lambda(k, V)$ at large $|k|$. In the classical continuum case ($\Lambda(k, V) = c^2 - V^2$) the sets M^\pm are empty, and the strain $w(\xi)$ is discontinuous at $\xi = 0$. In nonclassical quasicontinuum models considered in this paper and the discrete model with $q > 1$ $\Lambda(k, V)$ grows as $|k|^2$ or faster at large $|k|$. This leads to

$$\lim_{R \rightarrow \infty} \int_{|k|=R} \frac{dk}{k\Lambda(k, V)} = \lim_{R \rightarrow \infty} \int_{|k|=R} \frac{dk}{\Lambda(k, V)} = 0,$$

and hence the following residue sums are zero:

$$\frac{1}{c^2 - V^2} + \sum_{k \in M(V)} \frac{1}{k\Lambda_k(k, V)} = 0, \quad \sum_{k \in M(V)} \frac{1}{\Lambda_k(k, V)} = 0, \quad (44)$$

where $M(V) = M^+(V) \cup M^-(V)$ is the set of all roots of $\Lambda(k, V) = 0$. Equations (42), (43) and (44) imply that both $w(\xi)$ and $w'(\xi)$ are continuous at $\xi = 0$. In general, the solution is of class C^r at $\xi = 0$ if $k^{-r-1}\Lambda(k, V) = O(1)$ at large non-real $|k|$. In the degenerate case of discrete model with $q = 1$ (only NN interactions) one has $\Lambda^D(k, V) \approx 1$ at large non-real $|k|$. As a result, the contribution from a semi-arch closing the contour Γ in (40) at infinity does not vanish at $\xi = \pm 0$, and the relations (42), (43) must be supplemented by the limiting conditions [33]

$$w(\xi) = \begin{cases} w_- + \sum_{k \in M^-(V)} \frac{1}{k\Lambda_k(k, V)} - \frac{1}{2} & \text{for } \xi = -0 \\ w_+ - \sum_{k \in M^+(V)} \frac{1}{k\Lambda_k(k, V)} + \frac{1}{2} & \text{for } \xi = +0. \end{cases}$$

In this case the first residue sum in (44) equals 1, which together with the above conditions and (43) implies continuity of $w(\xi)$ at $\xi = 0$.

7 Kinetic relation

As indicated by (43), the strains w_\pm at infinity depend on the velocity V of the traveling wave. In fact, the continuity of strain at $\xi = 0$ and the phase switch condition (37) imply that

$$w_\pm = w_c \mp \frac{1}{2(c^2 - V^2)} + \sum_{k \in N_{\text{pos}}(V)} \frac{1}{|k\Lambda_k(k, V)|}, \quad (45)$$

where $N_{\text{pos}}(V) = \{k \in N^+(V) \cup N^-(V) : k > 0\}$ is the set of all positive real roots of $\Lambda(k, V) = 0$.

The analysis of the traveling wave solution (42), (45) demonstrates that a phase boundary moving through a lattice emits elastic waves that carry the energy away from the front without changing the average values of parameters at infinity. At the continuum level these lattice waves are invisible, and the associated energy transfer from long waves is perceived as dissipation. The rate \mathcal{R} of energy dissipation on the macrolevel

can be written as the sum of the contributions due to the fluxes of energy carried by the waves ahead and behind the phase boundary [12,33]:

$$\mathcal{R}(V) = \mathcal{R}_+(V) + \mathcal{R}_-(V). \quad (46)$$

To compute these contributions, we observe that due to the exponential decay of the modes with complex wave numbers, our solution (42) has the following asymptotic representation at large $|\xi|$:

$$w(\xi) \approx w_0(\xi) + \sum_{k \in N_{\text{pos}}(V)} w_k(\xi).$$

where

$$w_0(\xi) = \begin{cases} w_-, & \xi < 0 \\ w_+, & \xi > 0 \end{cases}$$

is the homogeneous component and

$$w_k(\xi) = \begin{cases} \frac{2 \cos(k\xi)}{k \Lambda_k(k, V)}, & \xi < 0, \quad k \in N_{\text{pos}}^-(V) \\ -\frac{2 \cos(k\xi)}{k \Lambda_k(k, V)}, & \xi > 0, \quad k \in N_{\text{pos}}^+(V) \end{cases} \quad (47)$$

are the oscillatory components (radiative modes). Here $N_{\text{pos}}^\pm(V) \equiv \{k \in N^\pm(V) : k > 0\}$, so that $N_{\text{pos}}^+(V) \cup N_{\text{pos}}^-(V) = N_{\text{pos}}(V)$. Due to the asymptotic orthogonality of the linear modes, the terms in the right hand side of (46) can be expressed as contributions due to individual modes. Since the energy flux associated with the linear mode k is the product of the average energy density $\langle \mathcal{G}_k \rangle$ and the relative speed $|V_g - V|$ of the energy transport with respect to the moving front, we can write

$$\mathcal{R}_+(V) = \sum_{k \in N_{\text{pos}}^+(V)} \langle \mathcal{G}_k \rangle_+ (V_g - V), \quad \mathcal{R}_-(V) = \sum_{k \in N_{\text{pos}}^-(V)} \langle \mathcal{G}_k \rangle_- (V - V_g). \quad (48)$$

Here $\langle \mathcal{G}_k \rangle_\pm$ is the average energy density carried by the wave with the wave number $k \in N_{\text{pos}}^\pm(V)$. It is given by

$$\langle \mathcal{G}_k \rangle_\pm = \lim_{n \rightarrow \pm\infty} \frac{1}{2V\tau(k)} \int_{n-V\tau(k)}^n (V^2 \mathcal{K}(k) + \mathcal{L}(k)) w_k^2(\xi) d\xi,$$

where $\tau(k) = 2\pi/\omega(k) = 2\pi/(Vk)$. Recalling that $\Lambda(k, V) = \mathcal{L}(k) - V^2 \mathcal{K}(k) = 0$ for $k \in N_{\text{pos}}^\pm(V)$ and using (47), we obtain

$$\langle \mathcal{G}_k \rangle_\pm = \frac{2V^2 \mathcal{K}(k)}{k^2 \Lambda_k^2(k, V)},$$

which, together with (41), gives for the total energy flux

$$\mathcal{R}(V) = V \left(\sum_{k \in N_{\text{pos}}^+(V)} \frac{1}{k \Lambda_k(k, V)} - \sum_{k \in N_{\text{pos}}^-(V)} \frac{1}{k \Lambda_k(k, V)} \right) = V \sum_{k \in N_{\text{pos}}(V)} \frac{1}{|k \Lambda_k(k, V)|}.$$

Recalling that $\mathcal{R}(V) = G(V)V$, we obtain the following expression for the driving force:

$$G(V) = \sum_{k \in N_{\text{pos}}(V)} \frac{1}{|k \Lambda_k(k, V)|} \quad (49)$$

Since the sets N_{pos} depend on V , (49) furnishes, although not in an explicit form, the desired kinetic relation between the driving force and the velocity of the moving boundary.

We observe that the formula (49) can also be obtained from the macroscopic assessment of dissipation (3), which can be interpreted geometrically as the difference between the shaded areas shown in Fig. 1. In the bilinear case we use the relations $\phi_+ = (1/2)c^2w_+^2$, $\phi_- = (1/2)c^2w_-^2 - w_- + w_c$, $\sigma_+ = c^2w_+$, $\sigma_- = c^2w_- - 1$ to obtain

$$G = \frac{1}{2}(w_- + w_+) - w_c. \quad (50)$$

Substituting (45) in (50), we expectedly recover (49).

8 Examples

To illustrate the general analysis presented in the previous sections, below we focus on a specific case of a lattice with $q = 2$ as the simplest nontrivial example of a lattice model accounting for bilinear local (nearest neighbor, or NN) and linear nonlocal (next to nearest neighbor, or NNN) interactions. In the nondimensional variables the model is fully characterized by a single dimensionless parameter $\beta = 4\Psi(2)/\Psi(1)$ measuring the relative strength of NNN interactions. The total energy of the system can be written as

$$\mathcal{E} = \sum_{n=-\infty}^{\infty} \left[\frac{\dot{u}_n^2}{2} + \frac{1+\beta}{2}w_n^2 - \theta(w_n - w_c)(w_n - w_c) - \frac{\beta}{4}(w_{n+1} - w_n)^2 \right]. \quad (51)$$

The macroscopic sound speed (11) reduces in this case to

$$c^2 = 1 + \beta. \quad (52)$$

For this discrete model one can obtain explicit traveling wave solutions describing the motion of an isolated phase boundary and present the kinetic relation in the form of a numerical procedure generating the function $G = G(V, \beta)$ [33].

Our task in what follows is to choose a quasicontinuum approximation which approximates this function best. Following [33], we limit our analysis to the interval

$$\beta_1 < \beta \leq 0, \quad (53)$$

where $\beta_1 \approx -0.9539$. The lower bound ensures the existence of a fast subsonic traveling wave solution with monotone leading edge and a single radiative mode behind the phase boundary, which will be the prime target of our modeling, while the upper bound is suggested by the linearization of the potentials of the Lennard–Jones type [30,31]. It is known that the kinetic relations generated by fully inertial lattice models are quite complex in the small velocity range due to a large number of lattice resonances [12,33]. Since the stability of a steadily moving isolated front in this regime is questionable (e.g. [33]), we intentionally leave it outside our quasicontinuum modeling.

8.1 Quadratic expansions

We begin by considering the simplest quadratic expansions in both SG and MG models. This corresponds to setting $\alpha_2 = 0$ in (25) and $a_2 = 0$ in (27); the first model will be called SG1 and the second one MG1. In both cases equation $\Lambda(k, V) = 0$ has two symmetric roots which are either real, $k = \pm r$, or purely imaginary, $k = \pm is$. When the roots are real the solution takes the form

$$w(\xi) = \begin{cases} w_c + \frac{1 - \cos(r\xi)}{c^2 - V^2} & \text{for } \xi < 0, \\ w_c & \text{for } \xi > 0, \end{cases} \quad (54)$$

and the kinetic relation then reduces to

$$G = \frac{1}{2(c^2 - V^2)}. \quad (55)$$

In the case of purely imaginary roots the (subsonic) solution takes the form

$$w(\xi) = \begin{cases} w_c + \frac{1 - e^{s\xi}}{2(c^2 - V^2)} & \text{for } \xi < 0 \\ w_c - \frac{1 - e^{-s\xi}}{2(c^2 - V^2)} & \text{for } \xi > 0. \end{cases} \quad (56)$$

The corresponding kinetic relation simply states that the dissipation is absent:

$$G = 0. \quad (57)$$

To be more specific, consider first the quadratic strain-gradient approximation (SG1 model). In this case we have

$$\Lambda(k, V) = c^2 - V^2 - \frac{1 + 4\beta}{12}k^2. \quad (58)$$

It is easy to see that at $V < c$ the roots of $\Lambda(k, V) = 0$ are real at $-1/4 < \beta \leq 0$ and imaginary otherwise. This implies that SG1 model predicts zero dissipation for $\beta < -1/4$ and is therefore unable to capture the phenomenon of radiative damping predicted in this parameter range by the lattice model. We observe that it is exactly the region where SG1 model is usually used (e.g. [28]) since it is uniformly well-posed there.

In the rest of the domain $-1/4 < \beta \leq 0$ the SG1 model predicts a nontrivial kinetic relation, although it can only be used if the real wavenumbers are in the interval $|k| \leq k_* = c\sqrt{12/(1 + 4\beta)}$. In this case there are two real roots of the dispersion relation and the formulas (54), (55) provide the solution of the problem.

In the MG1 approximation the dispersion relation takes the form

$$\Lambda(k, V) = c^2 - V^2 - \left(\frac{\beta}{4} + \frac{V^2}{12}\right)k^2. \quad (59)$$

In the interval $-1/4 < \beta \leq 0$ the MG1 model gives the same kinetics as SG1 model for $(-3\beta)^{1/2} < V \leq c$ and predicts zero dissipation for $V < (-3\beta)^{1/2}$. Like SG1 model, it is unable to capture radiative damping for $\beta < -1/4$ and predicts zero dissipation.

8.2 Comparison with discrete theory

The results of the numerical evaluation of the solutions of the quasicontinuum models are summarized in Fig. 2, where SG1 (dotted curves) and MG1 (dashed) approximations are compared to the discrete model in the interval $-1/4 < \beta \leq 0$. One can see that both SG1 and MG1 model overestimate the frequency and the amplitude of the radiation behind the front in the near-sonic domain (Fig. 2c). In addition, the approximations require the strain in front ($\xi > 0$) to be constant and equal to the critical value w_c , while in the discrete model the strain exponentially decreases to a finite value $w_+ < w_c$. Although at velocities sufficiently close to sonic limit the models capture the qualitative character of the discrete kinetic relation (see Fig. 2d), they overestimate the driving force.

Similar comparison in the interval $\beta < -1/4$ does not make much sense because both quasicontinuum models predict zero dissipation while the discrete theory generate a nontrivial kinetic relation (see Fig. 4). Overall, one can conclude that none of the quadratic models capture the discrete kinetics adequately in the whole range of parameters. To achieve a better approximation one needs to include higher order terms in the long-wave expansion, which is done in the next subsection.

8.3 Quartic approximations

If we keep fourth-order terms in our Taylor expansions, we obtain what we call SG2 model (25) and MG2 model (27). Assume as before (53) and subsonic V . With the exception of the interval $-1/16 < \beta \leq 0$, where SG2 model leads to four real roots, in both models the characteristic equation, $\Lambda(k, V) = 0$ has two real roots,

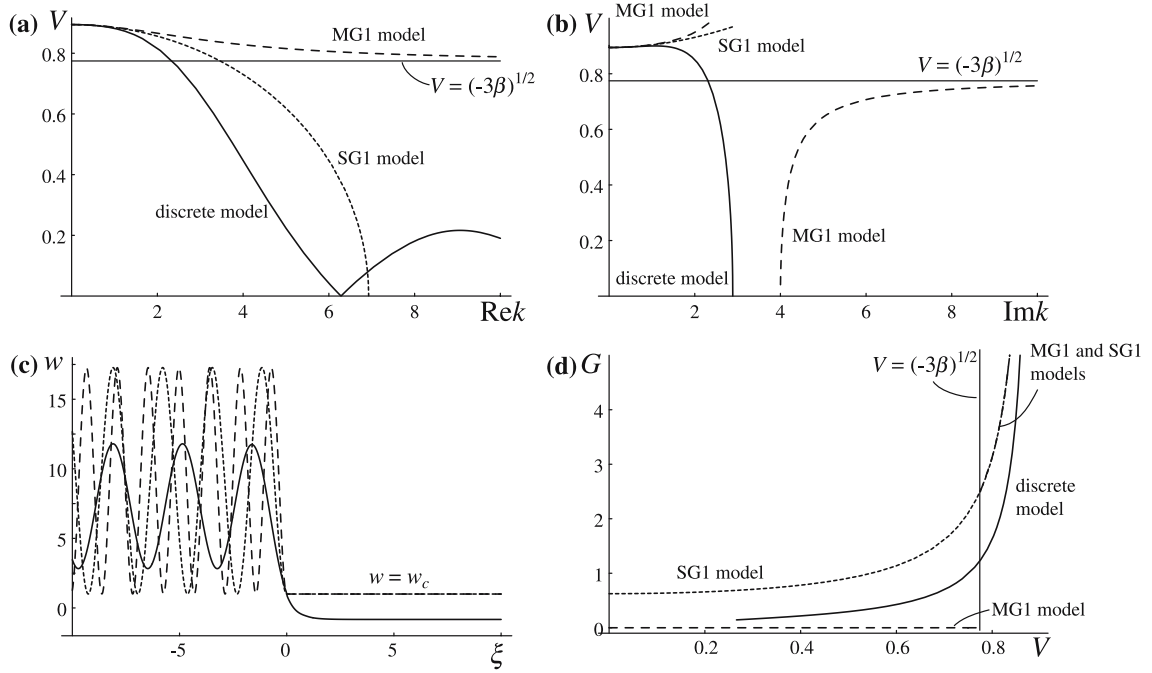


Fig. 2 Comparison of discrete (*solid curves*), MG1 (*dashed curves*) and SG1 (*dotted curves*) models at $-1/4 < \beta \leq 0$: the structure of **a** real and **b** imaginary roots; **c** strain profiles at $V/c = 0.92$, $w_c = 1$; **d** the mobility curves. In all pictures $\beta = -0.2$

$k_{1,2} = \pm r$, and two imaginary roots, $k_{3,4} = \pm ip$. The traveling wave solution (33) at subsonic velocities then reduces to

$$w(\xi) = \begin{cases} w_c + \frac{2p^2(1 - \cos(r\xi)) + r^2(1 - e^{p\xi})}{2(c^2 - V^2)(p^2 + r^2)} & \text{for } \xi < 0 \\ w_c + \frac{r^2(e^{-p\xi} - 1)}{2(c^2 - V^2)(p^2 + r^2)} & \text{for } \xi > 0 \end{cases} \quad (60)$$

The kinetic relation (49) takes the form

$$G = \frac{p^2}{2(c^2 - V^2)(p^2 + r^2)}. \quad (61)$$

To specialize these formulas to SG2 model, we observe that in our example

$$\Lambda(k, V) = 1 + \beta - V^2 - \frac{1 + 4\beta}{12}k^2 + \frac{1 + 16\beta}{360}k^4 = 0, \quad (62)$$

If $-1/16 < \beta \leq 0$ the characteristic equation has four real roots $k = \pm r_1$ and $k = \pm r_2$, $r_1 < r_2$. The roots $k = \pm r_1$ approximate the discrete radiation, whereas the roots $k = \pm r_2$ are an artifact of the polynomial expansion with a positive higher-order coefficient and do not have a discrete analog. Thus, SG2 model cannot be used in this interval. At $\beta = -1/16$ the model reduces to SG1 approximation.

Assume now that $\beta_1 < \beta < -1/16$. By solving the dispersion relation we obtain two imaginary roots $k = \pm ip$ and two real roots $k = \pm r$ with the magnitudes

$$p = \sqrt{-\frac{180}{1 + 16\beta} \left(\frac{1 + 4\beta}{12} + \sqrt{\left(\frac{1 + 4\beta}{12} \right)^2 - \frac{1 + 16\beta}{90}(1 + \beta - V^2)} \right)},$$

$$r = \sqrt{-\frac{180}{1 + 16\beta} \left(\sqrt{\left(\frac{1 + 4\beta}{12} \right)^2 - \frac{1 + 16\beta}{90}(1 + \beta - V^2)} - \frac{1 + 4\beta}{12} \right)}.$$

Observe that this approximation is valid (V is real) for real k satisfying $|k| \leq k_*$, where

$$k_* = \sqrt{\frac{15 + 60\beta - 3\sqrt{15}\sqrt{-1 - 32\beta - 16\beta^2}}{1 + 16\beta}}. \quad (63)$$

The explicit kinetic relation in the SG2 approximation takes the form

$$G(V) = \frac{1}{4(c^2 - V^2)} \left\{ 1 - \left(1 - \frac{8(1 + 16\beta)}{5(1 + 4\beta)^2} (c^2 - V^2) \right)^{-1/2} \right\}. \quad (64)$$

To obtain the kinetic relation in the mixed gradient approximation we first adopt it to our example and get

$$\Lambda = c^2 - V^2 - \left(\frac{\beta}{4} + \frac{V^2}{12} \right) k^2 + \left(\frac{\beta}{48} - \frac{V^2}{240} \right) k^4. \quad (65)$$

In this case $\beta \leq 0$ ensures that the characteristic equation always has two imaginary and two real roots. Their magnitudes are given by the formulas

$$p = \sqrt{2} \sqrt{\frac{-(15\beta + 5V^2) - \sqrt{-75\beta(4 + \beta) + 30(2 + 17\beta)V^2 - 35V^4}}{5\beta - V^2}},$$

$$r = \sqrt{2} \sqrt{\frac{15\beta + 5V^2 - \sqrt{-75\beta(4 + \beta) + 30(2 + 17\beta)V^2 - 35V^4}}{5\beta - V^2}}.$$

In this model the cutoff wavenumber is

$$k_* = \sqrt{6 + \frac{2\sqrt{3}(4 + \beta)}{\sqrt{-\beta(4 + \beta)}}}.$$

Note that it is greater than k_* for SG2 model given in (63) for all β where the latter is real, so that the domain of applicability of the mixed gradient approximation is wider than that of the strain gradient approximation. The kinetic relation (49) is given in the mixed gradient approximation by the following explicit formula:

$$G(V) = \frac{1}{4(c^2 - V^2)} \left(1 + \frac{\sqrt{5}(3\beta + V^2)}{\sqrt{-15\beta(4 + \beta) + 6(2 + 17\beta)V^2 - 7V^4}} \right). \quad (66)$$

Next consider the well-posed MG1/2 and MGP models defined in (30) and (31), respectively. For the MG1/2 model the characteristic equation is given by

$$\Lambda(k, V) = c^2 - V^2 - \left(\frac{\beta}{4} + \frac{V^2}{12} \right) k^2 - \frac{V^2}{240} k^4. \quad (67)$$

In MGP approximation we obtain

$$\Lambda(k, V) = \frac{1 + \beta + (1/12)(1 - 2\beta)k^2}{1 + (k^2/12)} - V^2 \left(1 + \frac{k^2}{12} \right). \quad (68)$$

The characteristic equation in both models has two real and two imaginary roots with

$$p = \sqrt{2} \sqrt{5 + \frac{\sqrt{5}\sqrt{45\beta^2 + 12V^2 + 42\beta V^2 - 7V^4} + 15\beta}{V^2}},$$

$$r = \sqrt{2} \sqrt{-5 + \frac{\sqrt{5}\sqrt{45\beta^2 + 12V^2 + 42\beta V^2 - 7V^4} - 15\beta}{V^2}}$$

for MG1/2 model and

$$p = \sqrt{6} \sqrt{2 + \frac{\sqrt{1 - 4\beta + 4\beta^2 + 12\beta V^2} + 2\beta - 1}{V^2}},$$

$$r = \sqrt{6} \sqrt{-2 + \frac{\sqrt{1 - 4\beta + 4\beta^2 + 12\beta V^2} + 1 - 2\beta}{V^2}}$$

for MGP model. The kinetic equations are again explicit taking the form

$$G(V) = \frac{3V^2}{\sqrt{9\beta^2 + (6/5)(2 + 7\beta)V^2 - (7V^4/5)(\sqrt{5}\sqrt{45\beta^2 + 6(2 + 7\beta)V^2 - 7V^4 - 15\beta - 5V^2})}}$$

for MG1/2 model and

$$G(V) = -\frac{3\beta}{1 + 4\beta(3V^2 + \beta - 1) - (1 + 4\beta)\sqrt{1 + 4\beta(3V^2 + \beta - 1)}}$$

for MGP model.

8.4 Comparison with discrete theory

We can now compute the solutions in quartic models explicitly and compare the approximate kinetic relations with the exact one for the discrete model (see [33]). The first series of results is summarized in Fig. 3a, b which compares in the interval $-1/4 < \beta < -1/16$ the following three models: discrete (solid curves), MG2 (dashed) and SG2 (dotted). One can see that MG2 model gives a much better approximation of both real and imaginary roots. Near-sonic strain profiles for all three models are juxtaposed in Fig. 3c. The profiles for discrete (solid curve) and MG2 (dashed) models nearly coincide, while the SG2 approximation (dotted) gives a noticeably larger amplitude and smaller frequency of radiation behind the front. The kinetic relations for both approximations are compared to each other and the discrete kinetics in Fig. 3d. As expected, the kinetic curve for MG2 model (dashed curve) is much closer to the discrete kinetic relation (solid) than the SG2 approximation (dotted curve).

Next consider the interval $\beta_1 < \beta < -1/4$. In this parameter range the positive real root corresponding to radiation behind the front is not close to $k = 0$, so that both SG2 and MG2 approximations cannot be expected to capture the discrete kinetics quantitatively. Nevertheless, as Fig. 4 illustrates, MG2 model (dashed curves) provides a substantially better approximation of the discrete model (solid curves) than the SG2 model (dotted curves) in terms of both the kinetic relations $G(V)$ and the near-sonic traveling wave profiles. Note in particular that the MG2 kinetic curve stays close to the discrete fast branch over the whole velocity range, while the SG2 curve deviates away from it significantly as V approaches c . Although MG2 approximation naturally becomes worse for higher $|\beta|$ (the roots corresponding to radiation move further away from zero), it remains significantly closer to the discrete curve than the SG2 approximation.

The better performance of MG2 model is due to the fact that it directly approximates $\Lambda^D(k, V)$ near $k = 0$ together with its first two derivatives, while SG2 model effectively replaces $4 \sin^2(k/2)$ in (15) by k^2 before expanding it in Taylor series. Even though the Taylor expansion is no longer valid at larger k , the optimal ‘‘tuning’’ of the function and its derivatives near $k = 0$ apparently results in a better agreement with the discrete theory in a broad range of wave lengths.

Next consider the well-posed version of the MG model which we referred to as MG1/2 and MGP approximations. The corresponding roots of the dispersion relations are presented in Figs. 5a,b and 6a,b for $\beta = -0.2$ and $\beta = -0.5$, respectively, which also compares them with the roots for the discrete problem. One can see that at smaller $|\beta|$ the MG1/2 model gives a slightly better prediction of the real roots than the MGP model, while at larger $|\beta|$ the opposite is true. The reason for this becomes clear when one observes that the error of MG1/2 approximation is $-\beta k^4/48 + O(k^6)$ and therefore the quality of approximation is getting better at β gets closer to zero. Meanwhile, the error for MGP model is independent of β (to the lowest order) but depends instead on the velocity $V^2 k^4/240 + O(k^6)$, so this approximation improves at smaller velocities for $|k|$ close to zero. Figures 5c and 6c compare the strain profiles in both models to the discrete case. One

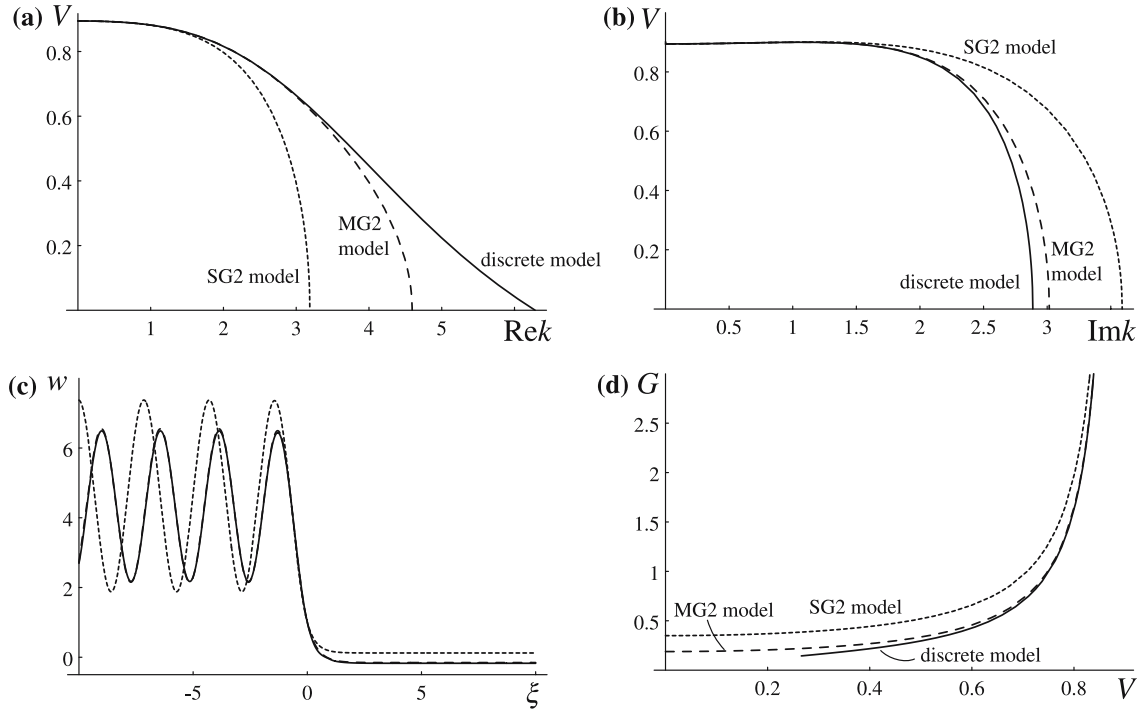


Fig. 3 Comparison of discrete (solid curves), MG2 (dashed curves) and SG2 (dotted curves) models at $-1/4 < \beta < -1/16$: the structure of **a** real and **b** imaginary roots; **c** strain profiles at $V/c = 0.85$, $w_c = 1$; **d** the mobility curves. In all pictures $\beta = -0.2$. In **c** the dashed and dotted curves nearly coincide

can see again that MG1/2 model works better at smaller β , while MGP model gives a better prediction of the discrete strain profile for larger β . Both models overestimate the frequency of radiation.

The kinetic relations generated by both models are compared with the discrete kinetics from [33] in Figs. 5d and 6d. As expected, kinetic relation for MG1/2 model is closer to the discrete one at smaller β (notice, however, that unlike the discrete model [33] it predicts $G(0) = 0$), and the MGP model gives a better prediction at higher $|\beta|$. Quite expectedly, both models give a worse approximation than MG2 model which is of higher order, but their advantage is that they are linearly stable at all wavelengths. In the next section we show how the best so far MG2 approximation can be adjusted to enjoy the same level of well-posedness.

9 Well-posed approximations

In constructing our quasicontinuum approximations we were guided so far exclusively by the desire to provide an optimal fit for the discrete dispersion relation at long waves. In order to be able to use the model outside the narrow framework of the traveling wave solutions, one needs to impose an additional condition that the model produces well-posed initial value problem. At least necessary conditions can be formulated quite easily. Indeed, we recall that the governing equations for all the approximate models considered so far are linear in each phase. Therefore to test the well-posedness of an initial value problem in the pure phases it is sufficient to consider the plane waves of the form $\exp[i(\omega t + kx)]$. The dispersion relation for a generic quasicontinuum approximation can be written as

$$\omega^2(k) = \frac{k^2 \mathcal{L}_A(k)}{\mathcal{K}_A(k)}, \quad (69)$$

where $\mathcal{L}_A(k)$ and $\mathcal{K}_A(k)$ are the corresponding approximations of $\mathcal{L}(k)$ and $\mathcal{K}(k)$. The wavenumbers k at which $\omega^2(k) < 0$ correspond to modes of instability for the homogeneous states away from the front. In view of (69) and the fact that $\mathcal{K}_A(k) > 0$ in all approximations considered above, these are the wavenumbers at which $\mathcal{L}_A(k) < 0$. For instance, if the coefficients in front of the highest-order term in $\mathcal{L}_A(k)$ are negative, homogeneous deformation is unstable with respect to perturbations with sufficiently short wave length, $|k| > k_*$, where

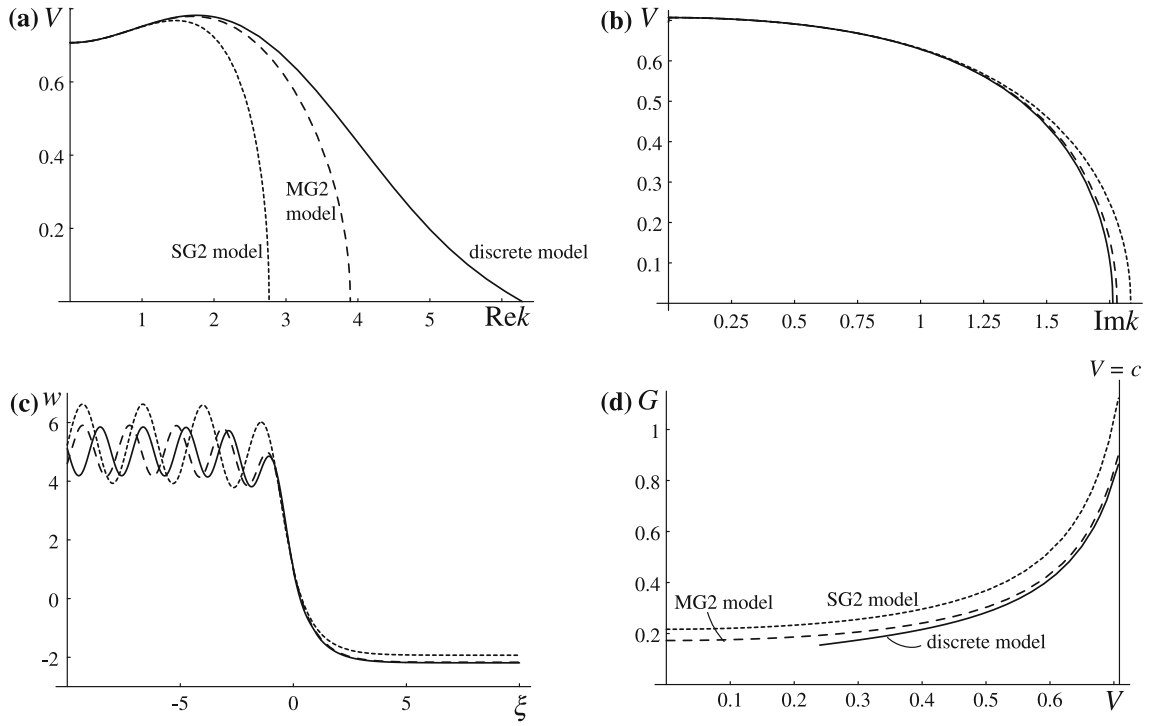


Fig. 4 Comparison of discrete (solid curves), MG2 (dashed curves) and SG2 (dotted curves) models at $\beta_1 < \beta < -1/4$: the structure of **a** real and **b** imaginary roots; **c** strain profiles at $V/c = 0.85$, $w_c = 1$; **d** the mobility curves. In all pictures $\beta = -0.5$

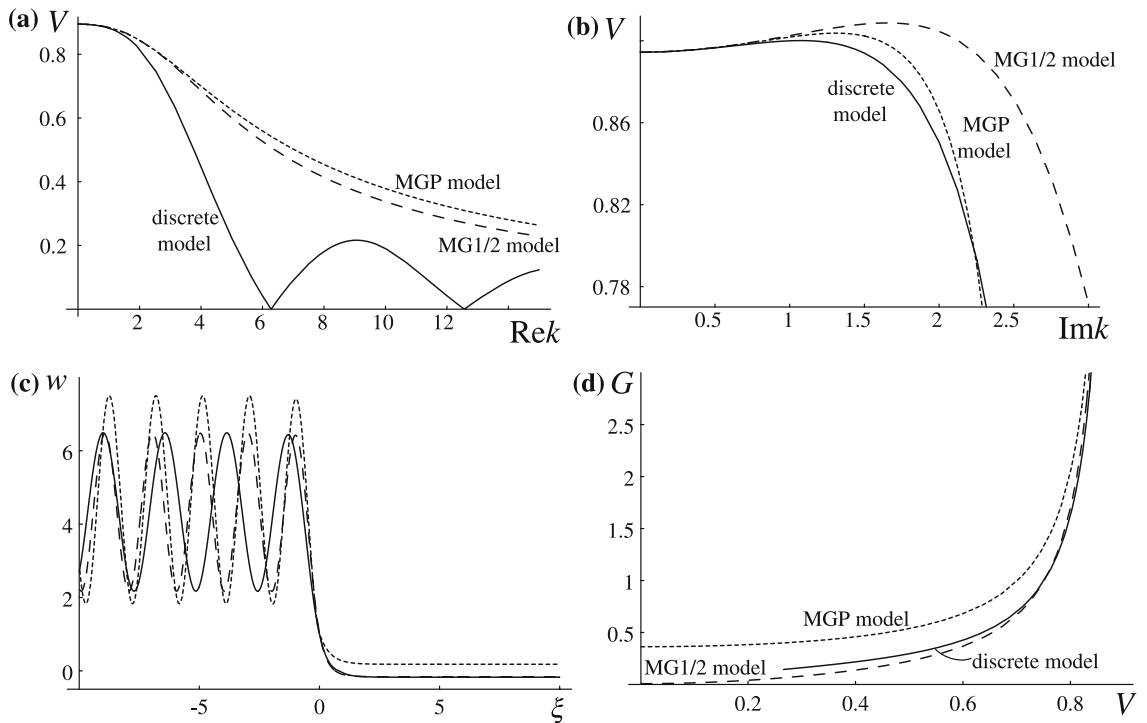


Fig. 5 Comparison of discrete (solid curves), MG1/2 (dashed curves) and MGP (dotted curves) models at $-1/4 < \beta \leq 0$: the structure of **a** real and **b** imaginary roots; **c** strain profiles at $V/c = 0.85$, $w_c = 1$; **d** the mobility curves. In all pictures $\beta = -0.2$

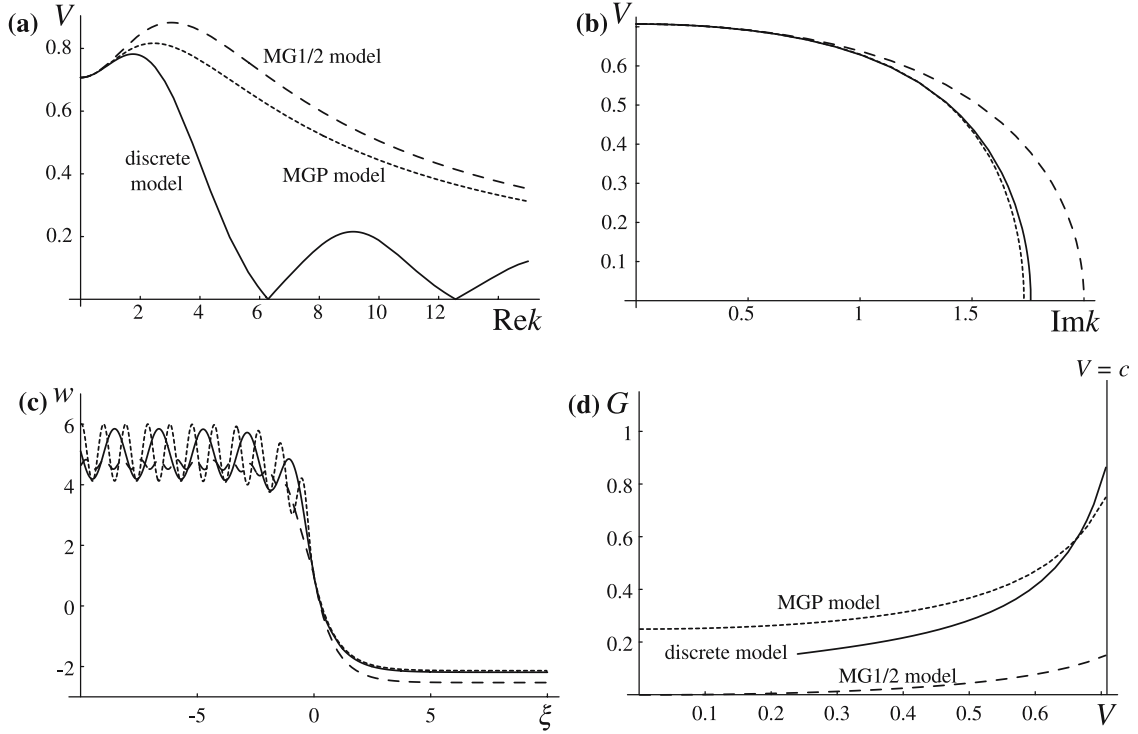


Fig. 6 Comparison of discrete (solid curves), MG1/2 (dashed curves) and MGP (dotted curves) models at $\beta_1 < \beta < -1/4$: the structure of **a** real and **b** imaginary roots; **c** strain profiles at $V/c = 0.85$, $w_c = 1$; **d** the mobility curves. In all pictures $\beta = -0.5$

$\mathcal{L}_A(k_*) = 0$. As one can readily see, this is indeed what happens with our “best” polynomial approximation (MG2 model) in at least one of the relevant parameter ranges.

Although this formally implies that this model is ill-posed, one has to keep in mind that the polynomial expansions are expected to be valid only for sufficiently long waves. The apparent short-wave instability is the result of the rigid, low parametric nature of the approximation and is unphysical given that the homogeneous deformation is stable in the original discrete problem. To eliminate this unphysical instability, the approximate models must be restricted to functions whose Fourier image is confined in the interval $|k| < k_*$ and the corresponding projection of the operator leads to a well-posed problem. In statics this restriction can be achieved by setting $\omega(k) = 0$ for real wave numbers that satisfy $|k| > \pi$ and thus correspond to length scales less than the lattice size [14, 34].

In dynamics we can similarly replace $\mathcal{L}(k)$ by

$$\mathcal{L}_\varepsilon(k) = \mathcal{L}_A(k) \eta_\varepsilon \left(\frac{k}{k_*} \right), \quad (70)$$

where $\varepsilon > 0$ is a small parameter, k_* satisfies $\mathcal{L}_A(k) = 0$ and

$$\eta_\varepsilon(y) = \frac{1}{2} \left(1 - \tanh \frac{y^2 - 1}{\varepsilon} \right) \quad (71)$$

is a smooth and analytic cut-off function, which is positive for all real y . Notice that for sufficiently small ε this function is close to one for $|y| < 1$ and decays exponentially fast to zero outside this interval. Thus for $|k| > k_*$ the function $\omega_\varepsilon^2(k) = k^2 \mathcal{L}_\varepsilon(k) / \mathcal{K}(k)$ is negative but approaches zero exponentially fast at large k . It tends to zero together with ε , so that the growth rate for short-wave instabilities also disappears in the limit. For real k one can show that $\eta_\varepsilon(k/k_*) \rightarrow \theta(1 - k^2/k_*^2)$ as ε tends to zero, effectively cutting off the unwanted wave-numbers. For instance, applying this procedure to the MG2 model we obtain in the limit $\varepsilon \rightarrow 0$ a *nonlocal* energy operator:

$$\mathcal{L}(k) \approx (c^2 + a_1 k^2 + a_2 k^4) \theta \left(1 - \frac{k^2}{k_*^2} \right) \quad (72)$$

In this case the quadratic part of the elastic energy takes the form

$$\frac{1}{2} \int_{-\infty}^{\infty} u_x \mathcal{L} u_x dx \approx \frac{1}{2} \int_{-\infty}^{\infty} \int_{-\infty}^{\infty} \Phi(x-y) u_x(x, t) u_x(y, t) dx dy,$$

where

$$\Phi(x) = \frac{1}{\pi x^5} \left\{ 2k_* x ((a_1 + 2a_2 k_*^2) x^2 - 12a_2) \cos(k_* x) + (24a_2 - 2(a_1 + 6a_2 k_*^2) x^2) \sin(k_* x) \right\}$$

is the oscillatory kernel that decays as $1/x^2$ at infinity. We remark that at sufficiently long waves the nonlocal approximation (72) of the potential energy operator is equivalent to the local gradient approximation (27)₂. The two models are expected to be close in at least some nonlinear regimes as well; in particular, they generate identical kinetic relations for all nonzero V .

10 Conclusions

In this paper we proposed a series of quasicontinuum approximations for the simplest one-dimensional lattice model describing dynamic martensitic phase transitions. The approximations are dispersive and include various non-classical corrections to both kinetic and potential energies. We showed that the quasicontinuum theory can be chosen in such a way that the associated closed-form kinetic relation is in excellent agreement with the predictions of the discrete theory for a broad range of phase boundary velocities. The essential ingredient making our approximations adequate in a wide range of parameters is the dispersive modification of the kinetic energy which introduces in the constitutive model the effects of micro-inertia. The presence of somewhat unusual kinetic energy terms at the mesoscale, where quasicontinuum models actually operate, reflects the oscillatory nature of the typical solutions in the discrete phase transition problem. To deal with the ill-posedness of the straightforward high-gradient quasicontinuum expansions we proposed to use a cutoff in the spectrum of the linearized operator. This operation, detailed in the paper, furnishes a canonical replacement of an ill-posed high-gradient model with a well-posed strongly nonlocal model with an explicit kernel. An unusual feature of this kernel is that the strong nonlocality of the model remains invisible in the case of long wave initial data until the nonlinearity is able to generate sufficiently short waves. The fact that this does not happen in the solutions describing isolated phase boundaries gives a hope that in most cases of interest one should be able to safely replace integral equations by partial differential equations. Future work is required to extend the proposed discrete and quasicontinuum models to account for microscopic dissipation represented by intrinsic viscosity, to cover simultaneously shock waves and phase boundaries and to deal with higher spatial dimensions. Another challenging problem is the analysis of the fully nonlinear model which allows for mixing of the radiated modes and subsequent thermalization.

Acknowledgements This work was supported by the National Science Foundation grants DMS-0102841 (L.T.), DMS-0137634 and DMS-0443928 (A.V.).

References

1. Abeyaratne, R., Knowles, J.: A continuum model of a thermoelastic solid capable of undergoing phase transitions. *J. Mech. Phys. Solids* **41**, 541–571 (1993)
2. Abeyaratne, R., Vedula, S.: A lattice-based model of the kinetics of twin boundary motion. *J. Mech. Phys. Solids* **51**, 1675–1700 (2003)
3. Benjamin, T.B., Bona, J.L., Mahony, J.J.: Model equations for long waves in nonlinear dispersive systems. *Phil. Trans. R. Soc. Lond.* **272**, 47–78 (1972)
4. Caflich, R.E., Miksis, M., Papanicolaou, G., Ting, L.: Wave propagation in bubbly liquid. *Lect. Appl. Math.* **23**, 327–343 (1986)
5. Collins, M.A.: A quasicontinuum approximation for solitons in an atomic chain. *Chem. Phys. Lett.* **77**, 342–347 (1981)
6. Gavriluk, S., Saurel, R.: Mathematical and numerical modeling of two-phase compressible flows with micro-inertia. *J. Comp. Phys.* **175**, 326–360 (2002)

7. Gustaffsson, B., Kreiss, H.O., Oliger, J.: Time-dependent Problems and Difference Methods. Pure and Applied Mathematics. Wiley, New York (1995)
8. Hochstrasser, D., Mertens, F.G., Büttner, H.: An iterative method for the calculation of narrow solitary excitations on atomic chains. *Phys. D* **35**, 259–266 (1989)
9. Kevrekidis, P.G., Kevrekidis, I.G., Bishop, A.R., Titi, E.S.: Continuum approach to discreteness. *Phys. Rev. E* **65**, 046,613 (2002)
10. Kevrekidis, P.G., Weinstein, M.I.: Dynamics of lattice kinks. *Phys. D* **142**, 113–152 (2000)
11. Kreiss, H.O., Busenhardt, H.U.: Time-dependent Partial Differential Equations and Their Numerical Solution. Lectures in Mathematics ETH Zürich. Birkhäuser Verlag, Basel (2001)
12. Kresse, O., Truskinovsky, L.: Mobility of lattice defects: discrete and continuum approaches. *J. Mech. Phys. Solids* **51**, 1305–1332 (2003)
13. Kresse, O., Truskinovsky, L.: Lattice friction for crystalline defects: from dislocations to cracks. *J. Mech. Phys. Solids* **52**, 2521–2543 (2004)
14. Kunin, I.: Elastic Media with Microstructure I: One-dimensional Models, Solid-State Sciences, vol. 26. Springer, Berlin Heidelberg New York (1982)
15. Lax, P.D., Levermore, C.D., Venakides, S.: The generation and propagation of oscillations in dispersive initial value problems and their limiting behavior. In: Fokas, A.S., Zakharov, V.E. (eds.) Important Developments in Soliton Theory, Springer Ser. Nonlin Dynam, pp. 205–241, Springer, Berlin Heidelberg New York (1994)
16. Marder, M., Gross, S.: Origin of crack tip instabilities. *J. Mech. Phys. Solids* **43**, 1–48 (1995)
17. Mindlin, R.D.: Second gradient of strain and surface tension in linear elasticity. *Int. J. Solids Struct.* **1**, 417–438 (1965)
18. Rayleigh, J.W.S.: The theory of sound, vol. I, II. Dover Publications, New York (1945)
19. Rogula, D.: Introduction to nonlocal theory of material media. In: Nonlocal Theory of material media, CISM Courses and Lectures, vol. 268, pp. 123–222, Springer, Wien (1982)
20. Rosenau, P.: Dynamics of nonlinear mass-spring chains near the continuum limit. *Phys. Lett. A* **118**(5), 222–227 (1986)
21. Rosenau, P.: Dynamics of dense discrete systems. *Prog. Theor. Phys.* **79**, 1028–1042 (1988)
22. Rosenau, P.: Hamiltonian dynamics of dense chains and lattices: or how to correct the continuum. *Phys. Lett. A* **311**(1), 39–52 (2003)
23. Sharma, B.L.: The kinetic relation of a Peierls dislocation in a higher-gradient dispersive continuum. Ph.D. Thesis, Cornell University (2004)
24. Slepyan, L.I.: Models and phenomena in fracture mechanics. Springer, Berlin Heidelberg New York (2002)
25. Slepyan, L.I., Cherkaev, A., Cherkaev, E.: Transition waves in bistable structures. II. Analytical solution: wave speed and energy dissipation. *J. Mech. Phys. Solids* **53**, 407–436 (2005)
26. Theil, F., Levitas, V.: A study of a hamiltonian model for martensitic phase transformations including microkinetic energy. *Math. Mech. Solids* **5**(3), 337–368 (2000)
27. Toupin, R.A.: Theories of elasticity with couple-stresses. *Arch. Ration Appl. Mech. Anal.* **17**, 85–112 (1964)
28. Triantafyllidis, N., Bardenhagen, S.: On higher order gradient continuum theories in 1-D nonlinear elasticity. Derivation from and comparison to the corresponding discrete models. *J. Elast.* **33**(3), 259–293 (1993)
29. Truskinovsky, L.: Dynamics of nonequilibrium phase boundaries in a heat conducting elastic medium. *J. Appl. Math. Mech.* **51**, 777–784 (1987)
30. Truskinovsky, L., Vainchtein, A.: Peierls–Nabarro landscape for martensitic phase transitions. *Phys. Rev. B.* **67**, 172,103 (2003)
31. Truskinovsky, L., Vainchtein, A.: The origin of nucleation peak in transformational plasticity. *J. Mech. Phys. Solids* **52**, 1421–1446 (2004)
32. Truskinovsky, L., Vainchtein, A.: Explicit kinetic relation from “first principles”. In: Steinmann, P. Maugin G. (eds.) *Mech Material Forces*, pp. 43–50, Springer, Berlin Heidelberg New York (2005)
33. Truskinovsky, L., Vainchtein, A.: Kinetics of martensitic phase transitions: lattice model. *SIAM J. Appl. Math.* **66**, 533–553 (2005)
34. Truskinovsky, L., Vainchtein, A.: Quasicontinuum modeling of short-wave instabilities in crystal lattices. *Philos. Mag.* **85**, 4055–4065 (2005)
35. Wattis, J.A.D.: Approximations to solitary waves on lattices, II: quasicontinuum methods for fast and slow waves. *J. Phys. A* **26**, 1193–1209 (1993)
36. Wattis, J.A.D.: Approximations to solitary waves on lattices, III: the monatomic lattice with second-neighbour interactions. *J. Phys. A* **29**, 8139–8157 (1996)
37. Wattis, J.A.D.: Stationary breather modes of generalized nonlinear Klein-Gordon lattices. *J. Phys. A* **31**, 3301–3323 (1998)